Title: Unresolved quenching mechanisms of chlorophyll fluorescence may invalidate multiple turnover saturating pulse analyses of photosynthetic electron transfer in microalgae

Authors: Vesa Havurinne, Heta Mattila, Mikko Antinluoma and Esa Tyystjärvi*

Department of Biochemistry / Molecular Plant Biology, University of Turku, FI-20014 Turku, Finland

*Corresponding author: esatyy@utu.fi, +358 2 333 5771

Abstract

Chlorophyll *a* fluorescence is a powerful tool for estimating photosynthetic efficiency, but there are still unanswered questions that hinder the use of its full potential. The present results describe a caveat in estimation of photosynthetic performance with so called rapid light curves with pulse amplitude modulation fluorometers. Rapid light curves of microalgae show a severe decrease in photosynthetic performance in high light, although a similar decrease cannot be seen with other methods. We show that this decrease cannot be assigned to energy dependent non-photochemical quenching or photoinhibition or to the geometry of the algal sample. The measured decrease in electron transfer rate is small in the tested siphonaceuous algae and higher plants, but very notable in all planktonic species, exhibiting species dependent variation in extent and reversibility. We performed in-depth analysis of the phenomenon in the diatom *Phaeodactylum tricornutum*, in which the decrease is the most pronounced and reversible among the tested organisms. The results suggest that quenching of fluorescence by oxidized plastoquinone alone cannot explain the phenomenon, and alternative quenching mechanisms within PSII need to be considered.

Abbreviations

Chl, chlorophyll; DCMU, 3-(3, 4-Dichlorophenyl)-1, 1-dimethylurea; DMF, N, N-dimethylformamide; ETR, electron transfer rate; F_M or F_M', maximum fluorescence of a dark acclimated or illuminated sample; FRRf, fast-repetition rate fluorometry; HL, high light; LC, light curve; MT, multiple turnover saturating pulse; MV, methyl viologen; NPQ, non-photochemical quenching; OD_{730}, light scattering at 730 nm; PAM, pulse amplitude modulation; PPFD, photosynthetic photon flux density; PQ, plastoquinone; PSI, Photosystem I; PSII, Photosystem II; rETR, relative electron transfer rate; RLC, rapid light curve; ST, single turnover saturating pulse; β, photoinhibition parameter; Φ_{II}, effective quantum yield of PSII

Introduction

Chlorophyll (Chl) *a* fluorescence is a powerful tool for the analysis of photosynthesis. A relationship between Chl *a* fluorescence yield and photosynthetic reactions was first described by Kautsky and Hirsch (1931), and presently chlorophyll fluorescence is a prime tool in studies of both structure and function of the photosynthetic apparatus (see e.g. Schreiber 2004, Tyystjärvi and Vass 2004, Baker 2008, Suggett et al. 2011, Kalaji et al. 2014, Porcar-Castell et al. 2014, Kalaji et al. 2017 for reviews).

In the early days of fluorescence measurements, most fluorometers were designed and tested with higher plants, but throughout the years there has been an increasing interest in estimating also the contributions of aquatic ecosystems to the global primary production using Chl fluorescence. In the heart of fluorescence measurements lies the effective quantum yield (Φ_{II}, also called YII, Y(II), $\Delta F/F_M$' or Genty parameter) of electron transfer through Photosystem II (PSII) that can be determined by a strong multiple turnover (MT) saturating pulse in e.g. pulse amplitude modulation (PAM) fluorometry, or by a sequence of multiple single turnover (ST) flashes used in fast-repetition rate fluorometry (FRRf). This quantum yield is the ratio of the increase in Chl *a* fluorescence yield from the value obtained under continuous illumination to the value obtained upon closing all PSII reaction centers (Genty et al. 1989). The ratio of variable to maximum fluorescence, measured from a dark-acclimated sample (Kitajima and Butler 1975), can be derived as a special case of the Genty parameter (Porcar-Castell et al. 2014).

The rate of electron transfer (ETR) is obtained by multiplying the quantum yield of PSII measured in the light by the number of photons absorbed by the PSII centers of the sample. One of the reasons why FRR fluorometers have become the predominant equipment for oceanographers is the fact that FRRf allows the estimation of the functional absorption cross-section of PSII from dilute algal samples (Suggett et al. 2011) and thereby estimation of the actual ETR of PSII. Although new and highly sensitive PAM fluorometers have been designed to accomplish similar estimations of absorption cross-section of PSII (Schreiber et al. 2012), these methods are not yet routinely used in PAM-applications, and relative ETR values (rETR) are often measured for comparison of effects of treatment or environmental condition on photosynthetic performance. The relationship between gas exchange measurements and fluorescence based ETR is more consistent in microalgae when using FRR fluorometers than PAM fluorometers (Suggett et al. 2003), but there are indications that also FRR based estimates of electron transfer deviate from linearity with gas exchange measurements at supraoptimal irradiance levels (Raateoja 2004).

In PAM fluorometry, the closure of all PSII reaction centers is typically achieved by firing a 0.3 to 1 s long pulse of high-intensity light. Because the maximum rate by which the cytochrome *b6f* complex removes electrons from the plastoquinone (PQ) pool is slower than the maximum delivery rate of electrons from PSII to the pool, the pool as well as the Q_A electron acceptor of PSII become transiently

reduced during the pulse. Maximum fluorescence (F_M or F_M') is measured when Q_A and the upstream electron transfer chain are fully reduced. A crucial problem in the actual measurements is that there is no easy way to routinely check if i) the saturating pulse actually leads to the closure of all PSII reaction centers of the sample and ii) the maximal fluorescence is not affected by quencher compounds such as oxidized PQ molecules (Kramer et al. 1995). Methods for correction of incomplete saturation have been designed, mainly to be used with plant material (Markgraf and Berry 1990, Earl and Ennahli 2004, Loriaux et al. 2013), but similar problems have also been noticed in cyanobacteria, where 3-(3, 4-Dichlorophenyl)-1, 1-dimethylurea (DCMU) is sometimes added to achieve full closure of PSII reaction centers (Campbell et al. 1998, Ogawa et al. 2017). Compared to F_M levels achieved by a strong ST pulse or a sequence of ST pulses fired in a short timeframe, the F_M values obtained by a MT pulse are usually higher (Koblížek et al. 2001). The differences between these two methods are also evident in the framework of polyphasic fast fluorescence induction kinetics, or OJIP curves (Strasser et al. 1995, Samson et al. 1999).

In ST flash approaches the fluorescence rise reaches only the intermediate fluorescence peak of the photochemical phase (O-J) of the fluorescence induction curve, whereas MT flash approaches also fulfill the requirements of the thermal phase of the fluorescence rise (J-I-P) and result in higher F_M values. The origin of the photochemical fluorescence rise phase of the OJIP curve is usually ascribed to represent mainly the reduction of Q_A (Kalaji et al. 2014), whereas the origin of the thermal phase is still debated (Stirbet and Govindjee 2012; Magyar et al. 2018). Both oxidized PQ molecules bound to PSII and free oxidized PQ are known quenchers of Chl fluorescence and the fluorescence rise during the thermal phase has traditionally been attributed to reduction of the PQ pool (Yaakoubd et al. 2002). For a long time, this PQ quenching has been the main explanation for the differences in F_M levels between ST and MT pulse approaches (Kramer et al. 1995, Suggett et al. 2003). Contesting views on what is causing the fluorescence rise during the thermal phase include conformational changes in PSII (Schansker et al. 2011; Magyar et al. 2018) and an increasing yield of fluorescence caused by P_{680}^+ $Pheo^-$ recombination reactions in closed PSII reaction centers (Schreiber and Krieger 1996).

In higher plants a good correlation usually exists between electron transfer rates estimated using the MT approach and other photosynthetic performance indicators like CO_2 fixation (Genty et al. 1989, Siebke et al. 1997), but discrepancies do occur also in plants at high incident irradiances (Li et al. 2014). In algae the light response of electron transfer rates measured using a traditional light curve (LC) approach shows a depression of rETR at supersaturating irradiances and does not resemble the actual light response of photosynthesis (Suggett et al. 2003, Beer and Axelsson 2004, Aikawa et al. 2009, Torres et al. 2014). This is especially true when the light acclimation steps are short, 10-60 s, as is the case in so called rapid light

curves (RLC). Elongation of the light steps to a time scale of minutes may in some cases result in removal of the artefactual decrease in ETR (Schreiber et al. 2012) but the use of long illumination steps is not a universal remedy (Beer and Axelsson 2004).

The decrease in ETR in fluorescence based RLCs in high light using the MT pulse approach has been addressed relatively early on (Suggett et al. 2003), yet a research culture of using RLCs still persists. We show that the magnitude and reversibility of the decrease in rETR is connected to the species under investigation and responds to culture conditions. We elaborate the physiological mechanism behind the phenomenon using the diatom *Phaeodactylum tricornutum* in extensive measurements carried out with the highly sensitive Multi-Color PAM fluorometer. Based on our results it is evident that fluorescence quenching by oxidized PQ molecules provides little explanatory power when compared to the magnitude of the phenomenon of decreasing rETR in high light intensities. Instead, the cause for the misestimates of rETR are likely located within the electron transfer chain of PSII reaction centers.

Materials and methods

Organisms

All organisms used in the current study were grown in conditions specifically optimized for each species. Algae (the green alga *Chlorella vulgaris* CCAP 211/11B and the diatom *P. tricornutum* CCAP 1055/1) and cyanobacteria (*Synechocystis* sp. PCC 6803, referred to as *Synechocystis* from here on) were cultured in 30-50 ml batches in mild shaking and only cells in the exponential phase were used for the experiments. *C. vulgaris* and *Synechocystis* were grown in BG-11 medium (Rippka et al. 1979) and *P. tricornutum* was grown in f/2 (modified from Guillard and Ryther 1962). The photosynthetic photon flux density (PPFD) of white light used for growing all algae and cyanobacteria was 40 μmol m^{-2} s^{-1}, while the red light (660 nm LED, Shenzen Led Fedy, Shenzen, China) conditions used to grow *P. tricornutum* cells with a lowered capacity to induce non-photochemical quenching of excitation energy (NPQ) were set to PPFD 43 μmol m^{-2} s^{-1} according to Schellenberger Costa et al. (2013). *P. tricornutum* was also grown in high light (HL; white light, PPFD 500 μmol m^{-2} s^{-1}) for certain experiments, but *P. tricornutum* grown in PPFD 40 μmol m^{-2} s^{-1} white light was used in the experiments unless otherwise specified. The HL grown *P. tricornutum* cultures were placed under 20 μmol m^{-2} s^{-1} of white light 2 h prior to the measurements in order to dissipate NPQ that was still remaining in the HL cultured cells immediately after taking them from HL conditions. The growth temperatures for *C. vulgaris*, *P. tricornutum* and *Synechocystis* were 25, 19 and 32°C, respectively, and all experiments were carried out at the growth temperature. The giant unicellular green alga *Acetabularia acetabulum* and the yellow-green filamentous alga *Vaucheria litorea* were grown in 12/12 h day/night cycle under PPFD 50 μmol m^{-2} s^{-1} of white light in 3.7 or 1% artificial

seawater (Tropic Marin Sea Salt Classic; Tropic Marin, Wartenberg, Germany), respectively, enriched with f/2 culture medium (Guillard and Ryther 1962). Growth temperature for *A. acetabulum* was 23°C and 17°C for *V. litorea*. Only healthy cells of similar size and age were used in the experiments for both macroalgae.

Arabidopsis thaliana WT (ecotype Columbia) and the NPQ deficient *npq1-2* mutant (Niyogi et al. 1998) plants were grown in short day conditions (8 h light/16 h dark) for 5-6 weeks before the experiments. Pumpkin (*Cucurbita maxima*, cv. Jättiläismeloni) was grown for 2 months in long day conditions (16 h light/8 h dark) before the isolation of functional thylakoids after 24 h dark acclimation as described by Hakala et al. (2005). The growth temperature was 22°C and the PPFD of white light was 150 μmol m^{-2} s^{-1} for all plants. All white light sources used for growing different species of algae, cyanobacteria or plants are listed on supplementary Table S1 (Appendix S1, Table S1).

Chlorophyll contents were quantified spectrophotometrically in methanol (*Synechocystis* and *C. vulgaris*) or buffered (pH 7.8) 80% acetone (plants) using the extinction coefficients by Porra et al. (1989), except for *P. tricornutum*, where Chl was quantified in N, N-dimethylformamide (DMF) using extinction coefficients for 90% acetone determined by Ritchie (2008). Extinction coefficients for 90% acetone have been shown to be suitable for approximate quantification of also DMF extracted Chl samples (Speziale et al. 1984).

Fluorescence measurements

The cell densities of all microalgae and cyanobacteria cultures were estimated spectrophotometrically by measuring light scattering at 730 nm (OD_{730}) and the OD_{730} of all samples was adjusted to 0.2 before the measurements, unless otherwise mentioned. The Chl concentrations of different species are naturally very variable, as for example in *Synechocystis* OD_{730}=0.2 corresponds to 0.42 μg Chl ml^{-1} in our culture conditions, whereas in the diatom *P. tricornutum* and the green alga *C. vulgaris*, the corresponding Chl concentrations are approximately 1.3 and 1.6 μg ml^{-1}, respectively. Multi-Color-PAM fluorometer (Heinz Walz GmbH, Effeltrich, Germany) was used for most fluorescence measurements with the following settings: low measuring light frequency 5000 Hz, high measuring light frequency 20000 Hz (automatically on during actinic light illumination), gain 3, damping 5. Measuring light intensity was adjusted for each species separately so that the initial fluorescence levels were comparable and a reliable signal was obtained. With the measuring light wavelength of 625 nm this meant adjustment between intensity settings 3-6. The actinic light wavelengths used in different experiments are specified in the results and discussion sections of the main text. All RLCs were measured from samples taken straight from their growth conditions, unless otherwise indicated.

Fluorescence was detected in the wavelength range of 650-710 nm unless otherwise stated. In one series of supplementary experiments a 680 nm bandpass filter (10 nm half width at half maximum; Newport Inc., Irvine, CA) was used to replace the manufacturer's filters in the detector unit of the PAM fluorometer to minimize the contribution of Photosystem I (PSI) fluorescence. In these experiments the measuring light intensity needed to be raised to intensity settings above 15 to obtain a reliable signal.

A standard protocol for measuring RLCs was used. Shortly, the sample was illuminated with a series of light intensities, starting from weak light and increasing the light intensity in a stepwise manner until a maximum. Each illumination step lasted 30 s, and at the end of the step, a saturating flash (0.8 s, PPFD = 10748 μmol m^{-2} s^{-1}) was fired to close PSII reaction centers for measuring the quantum yield of PSII. Relative electron transfer rate of PSII was calculated using the basic formula originally designed for plant material (rETR=Y(II) x incident PPFD x 0.84 x 0.5). In some measurements the sequence of light intensities was repeated in reverse after reaching the maximum light intensity to estimate the reversibility of the decrease in rETR (see Fig. 1 for an illustration of the method; this protocol will be called a reversible RLC). The maximum PPFD applied was 5-6 times as high as the PPFD that caused the maximum rETR. Deviations from the standard protocol are as indicated in the results section of the text. In the case of isolated pumpkin thylakoids, the RLC measurements were done in PSII measuring buffer (40 mM HEPES-KOH (pH 7.4), 1 M glycine betaine, 330 mM sorbitol, 5 mM $MgCl_2$, 5 mM NaCl, 1 mM KH_2PO_4 and 5 mM NH_4Cl) in the presence of 0.1 mM methyl viologen (MV) as an electron acceptor. The Chl concentration of the samples was 20 μg ml^{-1}.

Rapid light curve measurements in the presence of lincomycin were done with *P. tricornutum* cells in f/2 medium supplemented with 0.4 mg ml^{-1} of the antibiotic lincomycin using the reversible RLC protocol. Cells were incubated in the dark in lincomycin containing medium for 15 min before measurements and 480 nm actinic light was used in the experiments, as blue light induces photoinhibition in *P. tricornutum* more efficiently than other visible light wavelengths (Havurinne and Tyystjärvi 2017).

Another type of PAM-fluorometer, PAM-2000 (Heinz Walz GmbH, Effeltrich, Germany), was used for RLC measurements from *P. tricornutum* cells collected on a 1.2 μm glass fiber filter (VWR, Radnor, PA) with Chl concentration of 131 μg cm^{-2}. The filter was placed on a thermostated surface (19°C) covered in a cloth moistened with f/2 growth media and RLCs were measured using the standard protocol described above using the PAM-2000 halogen lamp for actinic light illumination. The same fluorometer and method was also utilized for standard RLC measurements from *A. thaliana, A. acetabulum* and *V. litorea*. In the case of the two macroalgae, cells were collected from growth conditions and placed on a paper towel moistened with f/2 medium as a uniform layer. Temperature was maintained at the growth temperatures of

the macroalgae. *A. thaliana* RLCs were measured at room temperature. The settings used in all PAM-2000 measurements were: saturating pulse intensity 10 (maximum), saturating pulse duration 0.8 s, low measuring light frequency 600 Hz, high measuring light frequency 20000 Hz (automatically on during actinic light illumination), gain 3, damping 5. Measuring light intensity was adjusted for each species separately between intensity setting 1-3 so that the fluorescence signals were comparable.

Oxygen evolution measurements

Oxygen evolution in the presence of 10 mM bicarbonate was measured simultaneously with fluorescence-based RLC from *P. tricornutum* cells by replacing the plug of the oxygen electrode cuvette with the fiber optics of PAM-2000. The connection was sealed with parafilm and the sample volume was adjusted to 2.2 ml. The OD_{730} of the sample was adjusted to 1, corresponding to roughly 6.5 μg Chl ml^{-1}. The rather high optical density of the sample in these experiments was a compromise between light attenuation and robust oxygen evolution traces. Also the duration of each illumination step of the RLC was increased to 1 min in order to obtain a reliable estimate of oxygen evolution during the steps. The samples were illuminated by the PAM-2000 halogen lamp through the fiber optics.

Inhibitor treatments

The photosynthetic electron transfer chain was inhibited in *P. tricornutum* by adding 10 μM DCMU prepared as dimethylsulfoxide stock solution (2 mM). DCMU was added 1 minute prior to the respective light treatment.

Results

Pattern of rapid light curves

The raw fluorescence responses of different species during a reversible RLC measurement protocol in white actinic light are shown in Fig. 1a. When rETR was calculated from the data, all measured organisms showed an increase of rETR to a maximum rETR and decrease with further increase in PPFD (Fig. 1b). During the immediate repetition of the PPFD sequence in reverse order, *A. thaliana* and *P. tricornutum* showed an almost perfect mirror image of the behavior of rETR, whereas *C. vulgaris*, *Synechocystis* and isolated pumpkin thylakoids showed a reduced increase in rETR when PPFD decreased toward the value that had produced the maximum rETR. The decrease in rETR between the PPFD producing the maximum, light saturated rETR and the maximum PPFD used was small in *A. thaliana* leaves but very large in all suspension samples (Fig. 1b). Interestingly, two macroalgae of very different evolutionary lineages, the green alga *Acetabularia acetabulum* and the yellow-green alga *Vaucheria litorea*, showed

little if any decrease in rETR in high actinic light intensities (Appendix S1, Fig. S1). Based on the finding that *P. tricornutum* exhibited both the largest amplitude and recovery from the decrease in rETR in supersaturating irradiances, we chose this alga for further studies.

Oxygen measurements show no decrease in ETR

To gain more insight into the question whether the decrease in rETR in light intensities exceeding saturation is a phenomenon reflecting changes in actual electron transfer rate or merely changes in fluorescence, we did RLC measurements using simultaneously oxygen evolution activity of PSII and fluorescence for estimating ETR in *P. tricornutum*. While fluorescence based RLCs clearly exhibited decrease of rETR when PPFD exceeded light saturation, there was no indication of this phenomenon in the oxygen evolution measurements (Fig. 2). Furthermore, the saturation of oxygen evolution occurred at PPFD >1410 µmol m^{-2} s^{-1} whereas fluorescence-based RLC measurements suggested saturation of rETR at PPFD 420 µmol m^{-2} s^{-1}. Similar discrepancies between O_2 evolution measurements and fluorescence based RLCs were noticed also in *Synechocystis* and isolated pumpkin thylakoid samples when these two parameters were measured separately (Appendix S1, Fig. S2).

Technical considerations of RLCs

Before proceeding to any detailed analysis of the decrease in rETR in high light, it was necessary to estimate the error that is inherent in the experimental procedure itself. We tested the correctness of our initial experimental protocol (i.e. saturating pulse intensity >10000 µmol photons m^{-2} s^{-1}, OD_{730}=0.2) by measuring RLCs from *P. tricornutum* with different saturating pulse intensities (Fig. 3a) and from different sample concentrations using the maximal intensity saturating pulse (Fig. 3b). Saturating pulse intensity did not have a dramatic effect on the shape of the RLC, as long as the PPFD of saturating pulse exceeded 3000 µmol m^{-2} s^{-1}, indicating that while it is important for the instrument to distinguish the fluorescence during the steady state fluorescence from fluorescence during the saturating pulse (F_M'), this is not the main reason behind the apparent decrease in rETR. This does not mean, however, that the convergence of these two fluorescence traces is not an issue, as it can be seen from the fluorescence traces on Fig. 1a, that the two tend to merge at very high intensity actinic light.

Sample concentration of an aqueous sample did have a clear effect on the RLCs, as the maximum rETR was reached at higher light in more concentrated samples. This behavior likely reflects the penetration of light into the sample. The rETR values increased with the optical density of the sample but decreased from OD_{730} 5 to OD_{730} 10, reflecting a complex interplay between increase in actual ETR with the number of cells in the sample, penetration of actinic light to the sample and self-absorption of emitted

fluorescence. However, the decrease in rETR in high light was noticeable in all tested sample concentrations, except for the most concentrated one.

The finding that the decrease of rETR in high light was noticeable in all tested aqueous samples of microalgae and even in isolated thylakoid membranes of pumpkins, but very unremarkable in plant leaves (Fig. 1b) or macroalgae (Appendix S1, Fig. S1), poses the question whether the decrease is related to the geometry of the samples, i.e. a truly three dimensional aqueous sample vs. an effectively flat surface of a leaf. To test this, a very high concentration of *P. tricornutum* cells (Chl concentration 184.6 μg cm^{-2}) were placed on a glass fiber filter and RLCs were measured with PAM-2000 fluorometer from a flat surface formed by the diatom cells. As was the case with Multi-Color PAM, also with PAM-2000 we could see a decrease in rETR in high light intensities, even in cells placed on a filter (Fig. 2c). Furthermore, *A. thaliana* leaves were found to behave similarly in Multi-Color PAM and PAM-2000, i.e. did not show a large decrease in rETR (data not shown), indicating that the phenomenon is neither geometrical nor instrumental origin.

Most Chl fluorescence originates from PSII at physiological temperatures, but a contribution of PSI fluorescence could interfere with the overall fluorescence signal and therefore be crucial in explaining the drop in rETR values in high light. Therefore we also tested the effect of PSI fluorescence to the RLCs in *P. tricornutum* and the green microalga *C. vulgaris*. While the normal Multi-Color PAM fluorescence detection range (650-710 nm) is already designed precisely for this purpose, we narrowed the range by replacing the original detector filters with a 680 nm bandpass filter to further reduce the contribution of PSI fluorescence. This modified protocol had no effect on the overall shape of the RLC measured from *P. tricornutum* or *C. vulgaris* in white light (Appendix S1, Fig. S3), indicating that the decrease of rETR in high light cannot be avoided by choosing a detector wavelength at the maximum of PSII fluorescence.

All data presented above indicate that the discrepancy between gas exchange measurements of ETR and fluorescence based rETR estimates (Fig. 2) is profound and cannot be easily dismissed by altering the measurement protocol of MT saturating pulse analysis of PAM fluorometers.

Photoinhibition and non-photochemical quenching

To test whether the decrease of rETR in supersaturating light is caused by irreversible photoinhibition of PSII during the high light phase, a reversible RLC was measured from lincomycin treated *P. tricornutum* cells using 480 nm actinic light. Lincomycin blocks the repair of PSII, and photoinhibition during the first high-light phase would therefore hinder the increase in rETR when light intensity is decreased from the maximum. However, reversible RLC measurements from lincomycin-treated *P. tricornutum* (Fig. 4a)

produced a similar mirror-image response as measurements in the absence of lincomycin (Fig. 1b), indicating that photoinhibition during the RLC measurement was negligible.

The relationship between NPQ and the high light decrease of rETR was investigated in *P. tricornutum* by utilizing the feature that this alga has a low NPQ capacity if grown in red light (Schellenberger Costa et al. 2013). Comparison of NPQ induction during an RLC measurement in *P. tricornutum* cells grown in white and red light confirmed low NPQ in the red-light culture. However, the RLC measurements in white actinic light produced very similar results irrespective of the NPQ capacity of the algae (Fig. 4b). The effect of NPQ on the decrease in rETR in high light was also estimated in *Synechocystis* under orange light (590 nm) that does not induce NPQ in *Synechocystis* (Kirilovsky and Kerfeld 2013), and in the NPQ deficient *npq1-2* mutant of *A. thaliana* (Niyogi et al. 1998). In neither of these cases did the deficiency in NPQ cause any significant effect on the overall shape of the RLCs (Appendix S1, Fig. S4).

High light acclimation dampens the amplitude of rETR decrease

The experiments presented so far show that the phenomenon of decreasing rETR in high light intensities does not mirror actual changes of PSII ETR (Fig. 2), but that the amplitude of the decrease differs in the tested organisms (Fig. 1). This suggests a physiological component behind the phenomenon. To test the physiological plasticity of the decrease within a single species, we grew *P. tricornutum* also in high light (HL; PPFD 500 µmol m^{-2} s^{-1} white light) and compared RLCs from these HL grown algae to those obtained previously from low light (LL) growth conditions, PPFD 40 µmol m^{-2} s^{-1}. The Chl concentration of HL grown cells was approximately half of that of LL grown cells (1.3 µg Chl ml^{-1} in LL cells and 0.7 µg Chl ml^{-1} in HL grown cells, normalized to OD_{730}), indicating a reduction in the antenna size of the HL grown cells as an acclimatory response to growth in high light. The same sample concentration (OD_{730} 0.2) was used for the HL grown algae as with the LL grown algae.

The RLCs were measured with 30 s illumination/PPFD, and different growth light conditions did affect the light utilization capabilities of *P. tricornutum*. Fig. 5 shows that $rETR_{MAX}$ of the HL cells is nearly twice as high as the $rETR_{MAX}$ value of the LL cells and also the saturation point of rETR (PPFD 455 and 851 µmol m^{-2} s^{-1} for LL and HL cells, respectively) has shifted to higher light intensities in the HL cells. The higher rETR value was likely not caused by the lower chlorophyll concentration of the HL sample, as the rETR values were found to decrease with decreasing chlorophyll concentration (Fig. 2b). Although clearly dampened in the HL acclimated cells, the decrease in rETR in supersaturating irradiances was still present and already noticeable at PPFD above 1000 µmol m^{-2} s^{-1} (Fig. 5).

Kinetics of rETR during light curves

We examined the kinetics of rETR in both LL and HL acclimated *P. tricornutum* cells by altering the durations of the actinic light illumination steps prior to firing the saturating pulses. First, we inspected the changes in fluorescence and rETR that take place immediately after switching on the supersaturating light. Here, a normal RLC protocol (i.e. 30 s of illumination/light intensity step prior to firing a MT saturating pulse) was implemented for the light limiting and light saturating steps, but after the onset of supersaturating light, the MT saturating pulses were fired every 5 s during the 30 s illumination period (Fig. 6a). One of the main concerns regarding the use of RLCs is the fact that the photosynthetic processes take minutes to acclimate to new light conditions, and therefore the fluorescence parameters measured during this acclimation process do not reflect the steady state physiology of the cells. Based on Fig. 6a, this argument seems to hold also for *P. tricornutum*, as the fluorescence trace is far from steady state after 30 s of PPFD 1898 µmol m^{-2} s^{-1} white light. The drop in rETR upon the onset of supersaturating light is immediate in both LL and HL grown cells, and similar kinetics were also noticed in *Synechocystis* cells and isolated pumpkin thylakoids (Appendix S1, Fig. S5). Both LL and HL cells reverted back to the rETR saturation levels when further treated with 30 s of rETR saturating light (PPFD 497 or 715 µmol m^{-2} s^{-1}, respectively). However, there is some indication in the HL cells that rETR responds to light acclimation processes and shows signs of increasing back to the saturation level of rETR already during the 30 s light treatment with PPFD 1898 µmol m^{-2} s^{-1} light. The LL grown cells did not show this kind of acclimation.

The extent of the acclimation process and its effect on the rETR values of LL and HL cells was estimated by increasing the supersaturating actinic light treatment from 30 s to 10 min while firing MT saturating pulses during the acclimation process (Fig. 6b). The elongated time step of 10 min was more than enough for the transient fluorescence to reach steady levels in HL cells, while a slight decline was noticeable throughout the high light treatment of LL cells. Regardless of the long acclimation period, the rETR values did not return to the rETR levels reached at light saturation point either in LL or HL cells, indicating that the slight rise in rETR in the HL cells of Fig. 6a is either i) simply a misestimate caused by the still rapidly declining fluorescence trace or ii) a very transient fluctuation in the acclimation status of the cells, lost when the light step is continued. Based on the finding that rETR of HL cells decreased to values below rETR saturation level when the actinic light was switched back to light saturation intensity for 30 s after the 10 min high light step, the second option seems more probable, as it indicates that at this stage rETR level is drastically affected by light acclimation status of the cells. In LL cells rETR returned back to saturation levels.

Next, we measured LCs from *P. tricornutum* by applying longer time steps with not just the supersaturating light intensities, but also with intensities that are light limiting and light saturating (Fig. 6c). Here achieving a moderately steady fluorescence level was the main criterion for the length of each

light step before firing a saturating pulse. Supersaturating light intensities (1119 and 1898 µmol m^{-2} s^{-1}) were continued for 10 min. Once again, the decrease of rETR was present in both LL and HL grown cells.

Fluorescence quenching caused by oxidized PQ

We probed the extent and behavior of PQ associated quenching during different intensities of actinic light illumination. Addition of DCMU blocks electron transfer from PSII reaction centers by binding to the Q_B site and therefore should lead to substantial oxidation of the photoactive PQ pool in an illuminated sample, allowing the estimation of the extent of fluorescence quenching by oxidized PQ molecules at different light intensities. This approach, however, does not allow to estimate the contribution of oxidized PQ molecules bound to PSII.

In LL grown *P. tricornutum* cells fluorescence quenching from the maximal level in the presence of DCMU was clear and the extent was similar in all tested light intensities (Fig. 7a), while the time required for reaching the full quenching potential positively correlated with increasing PPFD of the actinic light. When the kinetics of fluorescence quenching are inspected in more detail, it becomes clear that in light intensities exceeding PPFD 1000 µmol m^{-2} s^{-1} the quenching was nearly immediate (Fig. 7b). Interestingly, this type of quenching seems to be missing in high light grown *P. tricornutum*, at least in the PPFD range tested here (Fig. 7c,d). In addition to the quenching by oxidized PQ, a slower fluorescence quenching process was noticeable in both LL and HL grown samples under high irradiance when the illumination was continued (Fig. 7a,c). This type of quenching was more pronounced in the HL grown cells.

Discussion

On a partly sunny day the PPFD of natural sunlight fluctuates dramatically and can reach levels as high as 1500-2000 µmol m^{-2} s^{-1} at the water surface level (Huppertz et al. 1990, Torzillo et al. 2012). If fluorescence based RLCs presented in this work were to be taken at face value, the PSII electron transfer rate of *P. tricornutum* could be estimated to run only at approximately 60-90% capacity every time the clouds give way to full sun light. While photosynthetic performance is certainly affected by elongated exposure to light intensities as high as full sunlight, we have shown that the significant decrease in rETR witnessed in RLCs of multiple single celled organisms (Fig. 1) does not reflect the reality of electron transfer as measured by oxygen evolution (Fig. 2 and Appendix S1, Fig. S2), and therefore can lead to serious underestimations of primary production when MT fluorescence measurements are used as a proxy. While the phenomenon of decreasing electron transfer rates has often been dismissed as a minor flaw of

the measuring system, our results suggest that the phenomenon points to an actual physiological component of the photosynthetic apparatus.

The decrease in rETR persists in *P. tricornutum* even when the measurement conditions such as the concentration or dimensions (aqueous three-dimensional space or flat surface on a filter) of the sample, saturating pulse intensity or the measuring system are changed (Fig. 3). This indicates that the mechanisms behind the phenomenon are robust and allow comparison of results obtained from earlier work on the topic.

We were able to rule out some of the most obvious candidates that could be related to downplaying electron transfer through PSII in high light. We show that low rETR values measured in supersaturating light intensities do not reflect photoinhibition accumulating during the RLC measurement (Fig. 4a) and occur irrespective of the NPQ levels in different organisms (Fig. 4b and Appendix S1, Fig. S4). The distinction between photoinhibition and the decrease in rETR is of particular importance, as basic models of photosynthesis-irradiance curves contain a photoinhibition parameter β (Eilers and Peeters 1988) that becomes easily mixed with the decrease in rETR in supersaturating light.

Acclimation to high light could enhance the cells' capacity to run PSII efficiently in supersaturating light intensities and therefore diminish the decrease in rETR. To test this, we grew *P. tricornutum* in high light (PPFD 500 µmol m^{-2} s^{-1}) and measured RLCs from these cells. High light acclimation dampens the amplitude of the decrease in rETR in supersaturating light but does not remove the phenomenon (Fig. 5) or alter its fast induction kinetics (Fig. 6a). The differences in the behavior of rETR during a 30 s supersaturating light treatment, with HL cells showing some signs of adjustment and recovery of rETR at the end (Fig. 6a), might reflect different responses of the LL and HL cells to high light intensities. In the RLC of HL cells shown in Fig. 5 the short-term responses are likely lost during the successive light treatments before reaching the supersaturating light steps. This notion is also supported by our data showing that elongating the light steps from 30 s to minutes does not remove the decrease in rETR in LL or HL grown cells (Fig. 6b,c). Thus, use of long light steps is not a foolproof method that can be used to correct the misestimates of ETR in high light.

We tested the extent of fluorescence quenching caused by free oxidized PQ molecules during actinic light illumination by using DCMU to block electron transfer from PSII in LL and HL grown *P. tricornutum* cells. This resulted in a maximal fluorescence level that was then affected by oxidized PQ molecules. In the LL grown *P. tricornutum* cells a clear quenching effect was present after turning the actinic light on, even when the PPFD was as low as 38 µmol m^{-2} s^{-1}. The time requirement for the quenching to reach its full potential was affected by the PPFD of actinic light, and a saturation point was reached between 497

and 1119 µmol m^{-2} s^{-1} (Fig. 7a,b). In HL grown cells similar fast quenching was not noticeable, at least in the actinic light intensities tested here (up to 4835 µmol m^{-2} s^{-1}) (Fig. 7c,d). In both LL and HL grown cells the quenching continuously increased when the high actinic light treatment was continued (Fig. 7a,c). This slow, continuous quenching was most evident in the 4835 µmol m^{-2} s^{-1} actinic light treatments. Whether this type of continuous fluorescence quenching also affects fluorescence in the absence of DCMU remains unclear.

Fluorescence quenching in high light by different components of the photosynthetic electron transfer chain not directly related to the classical definition of NPQ has been known for decades. Such quenchers and associated phenomena include oxidized PQ molecules (Kramer et al. 1995, Samson and Bruce 1996), the oxidized primary donor P_{680}^{+} (Schreiber and Neubauer 1987), other chlorophyll cations (Schweizer and Brudwig 1997), influence of the electric field of the thylakoid membrane on redox reactions (Lebedeva et al. 2002), connectivity between PSII units (Joliot and Joliot 2003) and conformational changes within PSII (Schansker et al. 2011, Magyar et al. 2018). Reversal of the quenching by such factors in continuous high light is hypothesized to be the main cause behind the thermal phase of fluorescence induction (Stirbet and Govindjee 2012), and, by extension, also responsible for the differences in F_M levels reached during a ST or a MT saturating pulse (Suggett et al. 2003). The severity of these quenching phenomena to the analysis of overall photosynthetic performance should be kept in mind when using MT saturating pulse analyses. The ST based FRRf, where some of the quenchers have a smaller effect, has been shown to markedly improve estimates of photosynthesis in microalgae (Suggett et al. 2003).

Quenching of maximal fluorescence by oxidized PQ molecules during the closure of PSII reaction centers with ST, but not with MT pulses remains to be the most referred to explanation for the differences between ST and MT based estimates of photosynthetic electron transfer rate (Kramer et al. 1995, Samson and Bruce 1996, Stirbet and Govindjee 2012), making it a potential explanation also for the uncoupling of gas exchange and fluorescence based estimates of photosynthetic electron transfer (Fig. 2). However, the finding that decrease in rETR in high light is noticeable in HL grown *P. tricornutum* cells (Figs. 5 and 6), where fast fluorescence quenching by oxidized PQ molecules in the presence of DCMU is absent (Fig. 7 c,d), suggests that free oxidized PQ molecules of the PQ pool seem unlikely to be solely responsible for the decrease in rETR in supersaturating irradiances. Even in DCMU treated LL grown *P. tricornutum* cells, where PQ quenching was highly pronounced, the quenching resulted only in a minor decrease in fluorescence (Fig. 7 a,b) when compared to the decrease in rETR in similar incident irradiation (e.g. Fig. 5). Furthermore, oxidized PQ can explain the phenomenon only if the PQ pool becomes more reduced in light intensities that are supersaturating for PSII than at the saturating intensity.

Our results do not provide a basis for dismissing the role of PQ quenching in the high light decrease of rETR entirely. Instead, PQ quenching is likely one component of a set of reactions that result in a misestimate of rETR in high light, and other components need to be considered in order to improve fluorescence based estimates of primary production. Based on current literature it seems likely that the cause(s) behind the thermal phase of fluorescence induction and the misestimates of rETR in high light are intertwined. Recent findings in support of the hypothesis that light-induced conformational changes within PSII after full closure of the reaction centers are a major contributor to the thermal phase of fluorescence induction (Schansker et al. 2011; Magyar et al. 2018) provide a plausible explanation also for the uncoupling of fluorescence and gas exchange measurements of photosynthesis. The appeal of conformational changes within PSII as an explanation is enhanced because it can also account for many of the other suggested quenchers affecting the thermal phase, such as the oxidized primary donor $P680^+$ (Schreiber and Neubauer 1987). Changes in the preferred electron transfer routes within PSII might also have dramatic effects on the fluorescence yield. An interesting case of almost total uncoupling of fluorescence based estimates of PSII activity and oxygen evolution in microalgae is *Chlorella ohadii*, a green alga isolated from desert crust of Israel (Treves et al. 2013). The uncoupling of the two parameters in *C. ohadii* was assigned to the proposed cyclic electron flow pathway within PSII (Treves et al. 2013, Ananyev et al. 2017), a pathway suggested to participate in photoprotection in excess light also in the diatom *P. tricornutum* (Feikema et al. 2006).

Our findings have serious consequences for monitoring and modeling of aquatic primary production with PAM fluorescence or any other fluorescence method relying on MT saturating pulses. Firstly, although the phenomenon can be best seen in supersaturating light, comparison with oxygen evolution (Fig. 2) suggests that measurements at or below light saturation may be biased as well. In higher plant leaves the artefact is small even in very high light, but reliable rETR data cannot be obtained from microalgae or cyanobacteria with the simple MT saturating flash method. Based on the work by Beer and Axelsson (2004) also macroalgae are suspect, even though our results showed only slight decrease in rETR in the tested macroalgae species (Appendix S1, Fig. S1). With high resolution and high sensitivity equipment such as Multi-Color PAM, the underlying quenchers causing the misestimates of rETR can hopefully be resolved in the future. We have shown that *P. tricornutum* could be very helpful in such endeavors due to the plasticity of the phenomenon in this diatom. Using empirical coefficients to correct for the decrease in rETR would be one way of proceeding forward, but in the light of our findings this approach would not give satisfactory results unless the coefficients are tested for each species and light acclimation status separately. The present results show that the phenomenon of decreasing rETR in supersaturating light is an indicator of something real, and it would be a shame not to investigate this phenomenon's full potential in complementing the cornucopia of information that is already present in the fluorescence trace.

Author contributions

Experiments with *P. tricornutum* were carried out by VH. HM and MA did most of the experiments concerning other species in the study. ET supervised the project. VH, HM and ET designed the experiments. VH wrote the first draft of the manuscript and all authors participated in commenting and improving the text.

Acknowledgements

This work was supported by Academy of Finland, grant 307335 (ET), Nordforsk, Nordaqua project (ET), Turku University Foundation (HM), Finnish Cultural Foundation (VH) and the University of Turku Graduate School (UTUGS) (HM, VH). The *A. thaliana npq1-2* mutant seeds were a gift from Professor Krishna K. Niyogi.

References

Aikawa S, Hattori H, Gomi Y, Watanabe K, Kudoh S, Kashino Y, Satoh K (2009) Diel tuning of photosynthetic systems in ice algae at Saroma-ko Lagoon, Hokkaido, Japan. Polar Sci 3: 57-72

Ananyev G, Gates C, Kaplan A, Dismukes GC (2017) Photosystem II-cyclic electron flow powers exceptional photoprotection and record growth in the microalga Chlorella ohadii. Biochim Biophys Acta 1858:873-883

Baker NR (2008) Chlorophyll fluorescence: a probe of photosynthesis in vivo. Annu Rev Plant Biol 59: 89–113

Beer S, Axelsson L (2004) Limitations in the use of PAM fluorometry for measuring photosynthetic rates of macroalgae at high irradiances. Eur J Phycol 39: 1-7

Campbell D, Hurry V, Clarke AK, Gustafsson P, Öquist G (1998) Chlorophyll fluorescence analysis of cyanobacterial photosynthesis and acclimation. Microbiol Mol Biol Rev 62:667-683

Earl HJ, Ennahli S (2004) Estimating photosynthetic electron transport via chlorophyll fluorometry without photosystem II light saturation. Photosynth Res 82, 177–186

Eilers PHC, Peeters JCH (1988) A model for the relationship between light intensity and the rate of photosynthesis in phytoplankton. Ecol Modell 42: 199-215

Feikema WO, Marosvölgyi MA, Lavaud, J, van Gorkom HJ (2006) Cyclic electron transfer in photosystem II in the marine diatom Phaeodactylum tricornutum. Biochim Biophys Acta 1757: 829-834

503 Genty B, Briantais JM, Baker NR (1989) The relationship between quantum yield of photosynthetic
504 electron transport and quenching of chlorophyll fluorescence. Biochim Biophys Acta 990: 87-92

505 Guillard RRL, Ryther JH (1962) Studies of marine planktonic diatoms. I. Cyclotella nana Hustedt and
506 Detonula confervacea Cleve. Can J Microbiol 8: 229-239

507 Hakala M, Tuominen I, Keränen M, Tyystjärvi T, Tyystjärvi E (2005) Evidence for the role of the
508 oxygen-evolving manganese complex in photoinhibition of Photosystem II. Biochim Biophys Acta 1706:
509 68-80

510 Havurinne V, Tyystjärvi E (2017) Action spectrum of photoinhibition in the diatom Phaeodactylum
511 tricornutum. Plant Cell Physiol 58: 2217–2225

512 Huppertz K, Hanelt D, Nultsch W (1990) Photoinhibition of photosynthesis in the marine brown alga
513 Fucus serratus as studied in field experiments. Mar Ecol Prog Ser 66:175-182

514 Joliot P, Joliot A (2003) Excitation transfer between photosynthetic units: the 1964 experiment.
515 Photosynth Res 76: 241-245

516 Kalaji HM, Schansker G, Ladle RJ, Goltsev V, Bosa K, Allakhverdiev SI, Brestic M, Bussotti F,
517 Calatayud A, Dąbrowski P, Elsheery NI, Ferroni L, Guidi L, Hogewoning SW, Jajoo A, Misra AN,
518 Nebauer SG, Pancaldi S, Penella C, Poli DB, Pollistrini M, Romanowska-Duda ZB, Rutkowska B,
519 Serôdio J, Suresh K, Szulc W, Tambussi E, Yanniccari M, Zivcak M (2014) Frequently asked questions
520 about chlorophyll fluorescence: practical issues. Photosynth Res 122: 121–158

521 Kalaji HM, Schansker G, Brestic M, Bussotti F, Calatayud A, Ferroni L, Goltsev V, Guidi L, Jajoo A, Li
522 P, Losciale P, Mishra VK, Misra AN, Nebauer SG, Pancaldi S, Penella C, Pollastrini M, Suresh K,
523 Tambussi E, Yanniccari M, Zivcak M, Cetner MD, Samborska IA, Stirbet A, Olsovska K, Kunderlikova
524 K, Shelonzek H, Rusinowski S, Bąba W (2017) Frequently asked questions about chlorophyll
525 fluorescence, the sequel. Photosynth Res 132: 13-66

526 Kautsky H, Hirsch A (1931) Neue Versuche zur Kohlensäureassimilation. Naturwissenschaften 19: 964-
527 964

528 Kirilovsky D, Kerfeld CA (2013) The Orange Carotenoid Protein: a blue-green light photoactive protein.
529 Photochem Photobiol Sci 12: 1135-43

530 Kitajima M, Butler WL (1975) Quenching of chlorophyll fluorescence and primary photochemistry in
531 chloroplasts by dibromothymoquinone. Biochim Biophys Acta 376: 105–115

532 Koblížek M, Kaftan D, Nedbal L (2001) On the relationship between the non-photochemical quenching of
533 the chlorophyll fluorescence and the Photosystem II light harvesting efficiency. A repetitive flash
534 fluorescence induction study. Photosynth Res 68: 141-152

535 Kramer DM, Dimarco G, Loreto F (1995) Contribution of plastoquinone quenching to saturation pulse-
536 induced rise of chlorophyll fluorescence in leaves. In: Mathis P (ed) Photosynthesis from light to the
537 biosphere, vol 1. Kluwer Academic, Dordrecht, pp 147-150

538 Lebedeva GV, Beliaeva NE, Demin OV, Riznichenko G, Rubin AB (2002) Kinetic model of primary
539 processes of photosynthesis in chloroplasts. Fast phase of chlorophyll fluorescence induction under light
540 of various intensity. Biofizika 47: 1044-58

541 Li Q, Deng M, Yanshi X, Coombes A, Zhao W (2014) Morphological and photosynthetic response to
542 high and low irradiance of Aeschynanthus longicaulis. Sci World J 2014:1-8

543 Loriaux SD, Avenson TJ, Welles JJ, McDermitt DK, Eckles RD, Riensche B, Genty B (2013) Closing in
544 on maximum yield of chlorophyll fluorescence using a single multiphase flash of sub-saturating intensity.
545 Plant Cell Environ 36:1755-1770

546 Magyar M, Sipka G, Kovács L, Ughy B, Zhu Q, Han G, Špunda V, Lambrev PH, Shen J, Garab G (2018)
547 Rate-limiting steps in the dark-to-light transition of Photosystem II - revealed by chlorophyll-a
548 fluorescence induction. Sci Rep 8:2755

549 Markgraf T, Berry J (1990) Measurement of photochemical and non-photochemical quenching: correction
550 for turnover of PS2 during steady-state photosynthesis. In: Baltscheffsky M (ed) Current Research in
551 Photosynthesis. Springer, Dordrecht, pp 279-282

552 Niyogi KK, Grossman AR, Björkman O (1998) Arabidopsis mutants define a central role for the
553 xanthophyll cycle in the regulation of photosynthetic energy conversion. Plant Cell 10: 1121-1134

554 Ogawa T, Misumi M, Sonoike K (2017) Estimation of photosynthesis in cyanobacteria by pulse-
555 amplitude modulation chlorophyll fluorescence: problems and solutions. Photosynth Res 133: 63-73

556 Porcar-Castell A, Tyystjärvi E, Atherton J, van der Tol C, Flexas J, Pfündel EE, Moreno J, Frankenberg
557 C, Berry JA (2014) Linking chlorophyll a fluorescence to photosynthesis for remote sensing applications:
558 mechanisms and challenges. J Exp Bo. 65: 4065-4095

559 Porra RJ, Thompson WA, Kriedemann PE (1989) Determination of accurate extinction coefficients and
560 simultaneous equations for assaying chlorophylls a and b extracted with four different solvents:

verification of the concentration of chlorophyll standards by atomic-absorption spectroscopy. Biochim Biophys Acta 975: 384-394

Raateoja M (2004) Fast repetition rate fluorometry (FRRF) measuring phytoplankton productivity: A case study at the entrance to the Gulf of Finland, Baltic Sea. Boreal Env Res 9: 263-276

Rippka R, Deruelles J, Waterbury JB, Herdman M, Stanier RY (1979) Generic assignment, strain histories and properties of pure cultures of cyanobacteria. J Gen Microbio. 111: 1-61

Ritchie RJ (2008) Universal chlorophyll equations for estimating chlorophylls a, b, c, and d and total chlorophylls in natural assemblages of photosynthetic organisms using acetone, methanol, or ethanol solvents. Photosynthetica 46: 115-126

Samson G, Bruce D (1996) Origins of the low yield of chlorophyll a fluorescence induced by single turnover flash in spinach thylakoids. Biochim Biophys Acta 1276: 147-153

Schansker G, Tóth SZ, Kovács L, Holzwarth AR, Garab G (2011) Evidence for a fluorescence yield change driven by a light-induced conformational change within photosystem II during the fast chlorophyll a fluorescence rise. Biochim Biophys Acta 1807: 1032-1043

Schellenberger Costa B, Jungandreas A, Jakob T, Weisheit W, Mittag M, Wilhelm C (2013) Blue light is essential for high light acclimation and photoprotection in the diatom Phaeodactylum tricornutum. J Exp Bot 64: 483-493

Schreiber U, Neubauer C (1987) The polyphasic rise of chlorophyll fluorescence upon onset of strong continuous illumination: II. Partial control by the Photosystem II donor side and possible ways of interpretation. Z Naturforsch 42: 1255–1264

Schreiber U, Krieger A (1996) Two fundamentally different types of variable chlorophyll fluorescence in vivo. FEBS Lett 397: 131-135

Schreiber U (2004) Pulse-amplitude-modulation (PAM) fluorometry and saturation pulse method: an owerview. In: Papageorgiou G, Govindjee (eds) Chlorophyll *a* Fluorescence: A signature of photosynthesis. Advances in Photosynthesis and Respiration v 19. Springer, Dordrecht, pp 279-319

Schreiber U, Klughammer C, Kolbowski J (2012) Assessment of wavelength-dependent parameters of photosynthetic electron transport with a new type of multi-color PAM chlorophyll fluorometer. Photosynth Res 113: 127-144

589 Schweizer RH, Brudvig GW (1997) Fluorescence quenching by chlorophyll cations in Photosystem II.
590 Biochemistry 36: 11351–11359

591 Siebke K, Von Caemmerer S, Badger M, Furbank RT (1997) Expressing an RbcS antisense gene in
592 transgenic Flaveria bidentis leads to an increased quantum requirement for CO_2 fixed in photosystems I
593 and II. Plant Physiol 115: 1163-1174

594 Speziale BJ, Schreiner SP, Giammatteo PA, Schindler JE (1984) Comparison of N,N-dimethylformamide,
595 dimethylsulfoxide, and acetone for extraction of phytoplankton chlorophyll. Can J Fish Aquat Sci 41:
596 1519-1522

597 Stirbet A, Govindjee (2012) Chlorophyll *a* fluorescence induction: a personal perspective of the thermal
598 phase, the J-I-P rise. Photosynth Res 113:15-61

599 Strasser RJ, Srivastava A, Govindjee (1995) Polyphasic chlorophyll *a* fluorescence transient in plants and
600 cyanobacteria. Photochem Photobiol 61:32–42

601 Suggett DJ, Oxborough K, Baker NR, Macintyre HL, Kana TM, Geider RJ (2003) Fast repetition rate and
602 pulse amplitude modulation chlorophyll a fluorescence measurements for assessment of photosynthetic
603 electron transport in marine phytoplankton. Eur J Phycol 38: 371-384

604 Suggett DJ, Moore CM, Geider RJ (2011) Estimating aquatic productivity from active fluorescence
605 measurements. In: Suggett DJ, Prasil O, Borowitzka MA (eds) Chlorophyll a fluorescence in aquatic
606 sciences: Methods and applications, v 4. Springer, Dordrecht, pp 103-127

607 Torres MA, Ritchie RJ, Lilley RM, Larkum AW (2013) Measurement of photosynthesis and
608 photosynthetic efficiency in two diatoms. NZ J Bot 52: 6-27

609 Torzillo G, Faraloni C, Silva AM, Kopecký J, Pilný J, Masojídek J (2012) Photoacclimation of
610 Phaeodactylum tricornutum (Bacillariophyceae) cultures grown outdoors in photobioreactors and open
611 ponds. Eur J Phycol 47:169-181

612 Treves H, Raanan H, Finkel OM, Berkowicz SB, Keren N, Shotland Y, Kaplan A (2013) A newly isolated
613 Chlorella sp. from desert sand crusts exhibits a unique resistance to excess light intensity. FEMS
614 Microbiol Ecol 86:373-380

615 Tyystjärvi E, Vass I (2004) Light emission as a probe of charge separation and recombination in the
616 photosynthetic apparatus: relation of prompt fluorescence to delayed light emission and

thermoluminescence. In Papageorgiou G, Govindjee (eds) Chlorophyll *a* Fluorescence. Advances in Photosynthesis and Respiration, v 19. Springer, Dordrecht, pp 363-388

Yaakoubd B, Andersen R, Desjardins Y, Samson G (2002) Contributions of the free oxidized and Q_B-bound plastoquinone molecules to the thermal phase of chlorophyll-a fluorescence. Photosynth Res 74: 251

Supporting information

Additional supporting information may be found in the online version of this article:

Appendix S1. Supplementary Table S1 and Figs S1-S5

Figure legends

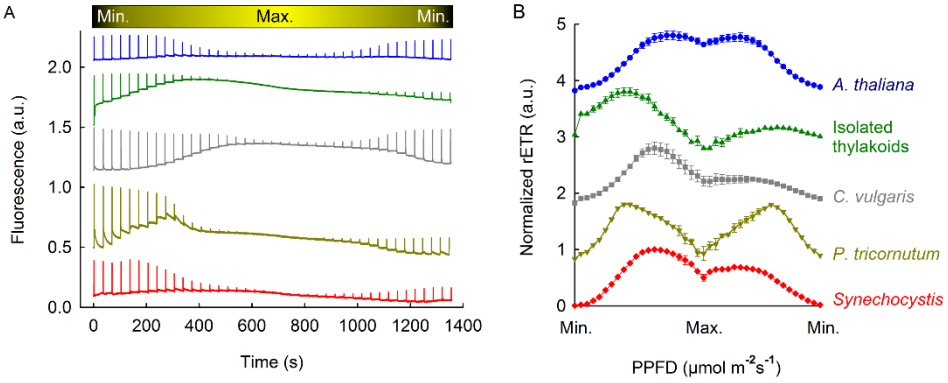

Fig. 1. Patterns of RLC measurements in white actinic light. a) Representative fluorescence traces during the RLC measurements from *A. thaliana* (blue), isolated pumpkin thylakoids (green), *C. vulgaris* (gray), *P. tricornutum* (dark yellow) and *Synechocystis* (red). The top bar shows the pattern of increase and decrease in light intensity. b) rETR values calculated from measurements shown in panel a. To facilitate comparison, all rETR values were normalized to their respective maxima and shifted in y-axis direction and the x-axis scale does not reflect the actual increments in PPFD, but the saturating pulse time points. The maximum PPFD range was 1500 to 4000 µmol m^{-2} s^{-1}, depending on the species. The RLC of isolated thylakoids was measured in the presence of 0.1 mM MV. Each RLC represents an average of three independent experiments and error bars, shown only if larger than the respective symbol, indicate SD.

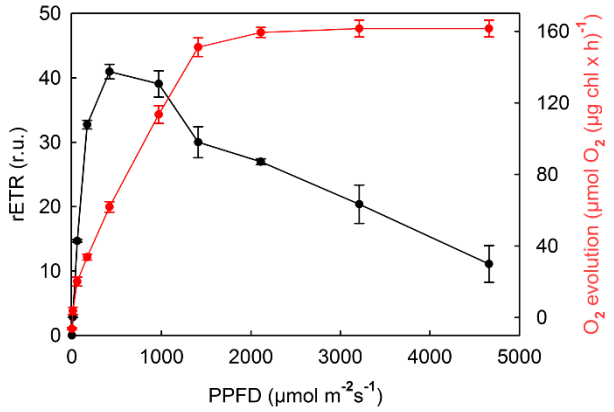

636

637 Fig. 2. Fluorescence based RLC (black circles) and light response of photosynthetic oxygen evolution (red
638 circles) in the presence of 10 mM bicarbonate in *P. tricornutum*. Both curves were measured
639 simultaneously from the same sample and the duration of the light steps was 60 s. Each data point
640 represents an average of three independent measurements and the error bars indicate SD.

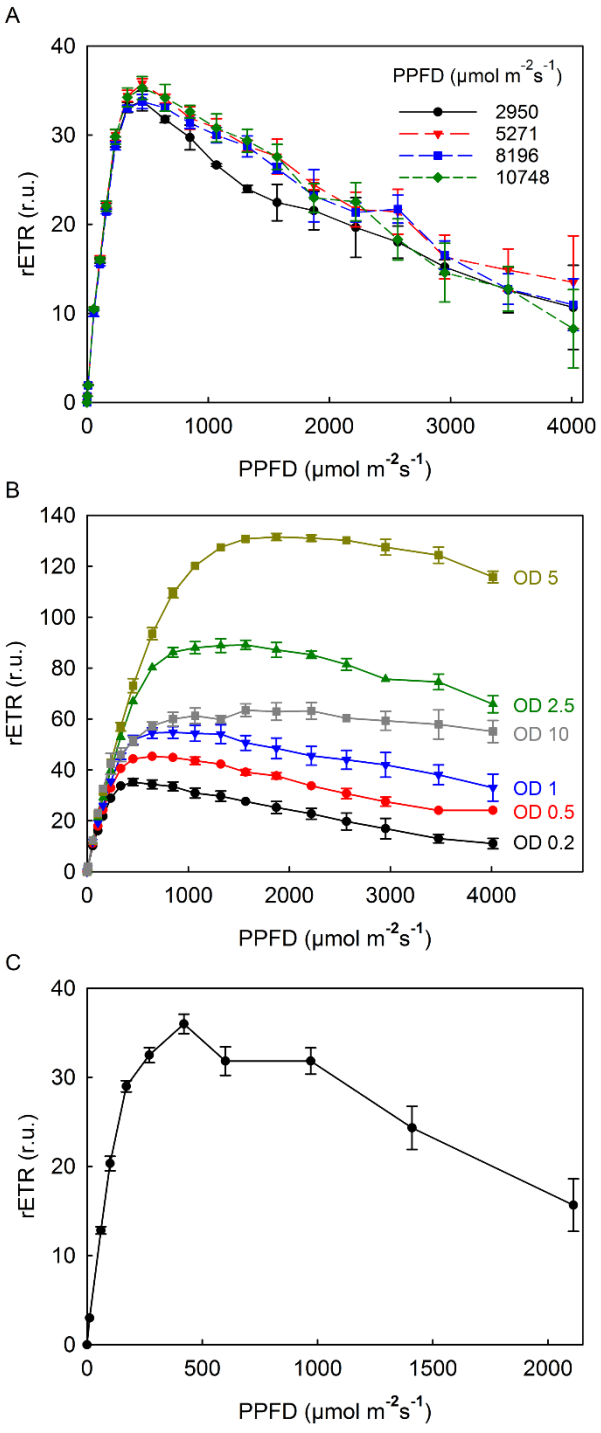

Fig. 3. Technical aspects affecting RLCs in *P. tricornutum*. a) The effect of saturating pulse intensity on RLCs. The intensity of the saturating pulses is indicated in the figure. b) RLCs measured from different sample concentrations. OD indicates light scattering at 730 nm (OD_{730}), reflecting the cell density of the samples. c) RLCs of *P. tricornutum* cells placed on a filter moistened with f/2 culture medium with a final

Chl concentration of 184.6 µg cm^{-2} measured with PAM-2000. Each data point represents an average of three independent measurements and the error bars indicate SD.

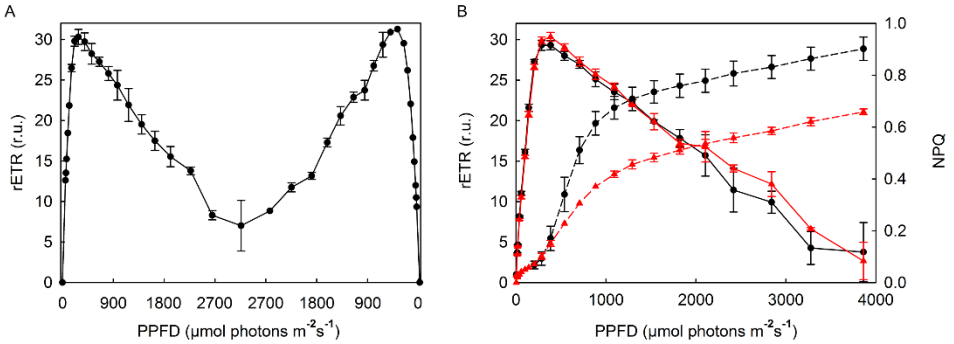

Fig. 4. a) Reversible RLC of lincomycin treated *P. tricornutum*. The algae were incubated in the dark in f/2 growth medium containing lincomycin (0.4 mg ml^{-1}) for 15 min before the measurements. 480 nm light was used as actinic light. b) RLCs (solid lines) and NPQ (dashed lines) from white light grown (black circles) and NPQ deficient red light grown (red triangles) *P. tricornutum* cells measured in white actinic light after 15 min dark acclimation. NPQ was calculated as $[F_M - F_M']/F_M'$. All data points represent an average of three independent replicates, and the error bars indicate SD.

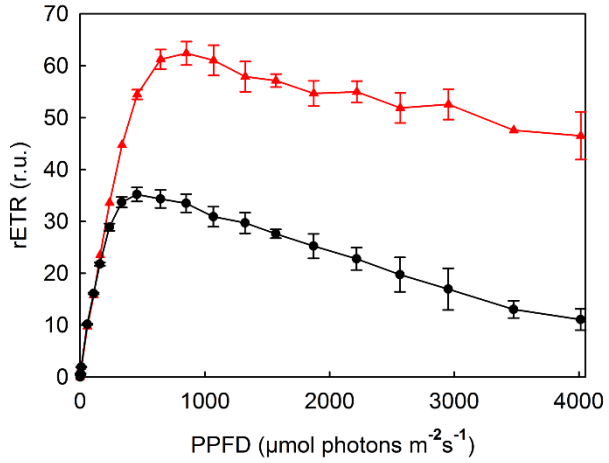

Fig. 5. The effect of light acclimation status of *P. tricornutum* on the decrease in rETR in high light intensities in regular RLC measurements. Black circles, low light grown cells (PPFD 40 µmol m^{-2} s^{-1}); red triangles, high light grown cells (PPFD 500 µmol m^{-2} s^{-1}). High light grown cells were illuminated with 20 µmol m^{-2} s^{-1} of white light for 2 h prior to the measurements. OD_{730} was 0.2 for both samples. All curves are averages from three independent replicates and the error bars indicate SD.

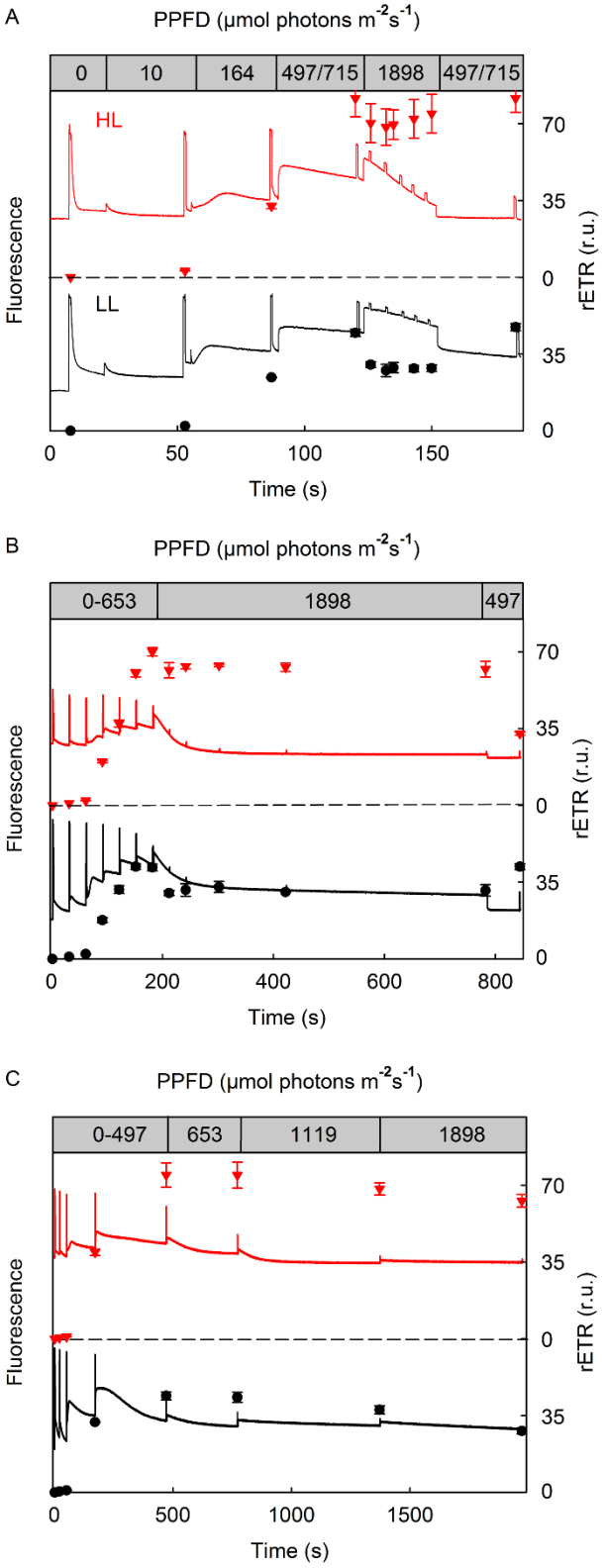

Fig. 6. Kinetics of rETR during light curves in low light (LL, black curves and black symbols in the lower section of the figures) and high light (HL, red curves and red symbols in the upper section of the figures)

acclimated *P. tricornutum* cells. Light intensities during different times of the measurements are shown in the upper grey bars. a) Kinetics of rETR (symbols) and fluorescence yield (lines) during 30 s of high intensity white light after the RLC has reached the saturation point of rETR. Saturation of rETR was achieved by 30 s of PPFD 497 or 715 µmol m^{-2} s^{-1} light treatment for the LL and HL acclimated cells, respectively, and the corresponding light intensities were used also at the end of the treatment to probe the recovery kinetics of rETR from the high light treatments. b) Kinetics of rETR and fluorescence during a transition from RLC (30 s/PPFD step) to LC (600 s/PPFD step) in high light after reaching a saturation point of rETR using a regular RLC protocol up to PPFD 653 µmol m^{-2} s^{-1}. Recovery from the decrease of rETR in high light was probed at the end by an additional 30 s of 497 µmol m^{-2} s^{-1} of white light. c) Kinetics of rETR during an LC, where the saturation pulse analysis was performed only after reaching a moderately steady fluorescence level at each light intensity step. All fluorescence curves in a), b) and c) are representative curves from individual measurements. All rETR data points in a), b) and c) are averages from three independent experiments and the error bars indicate SD.

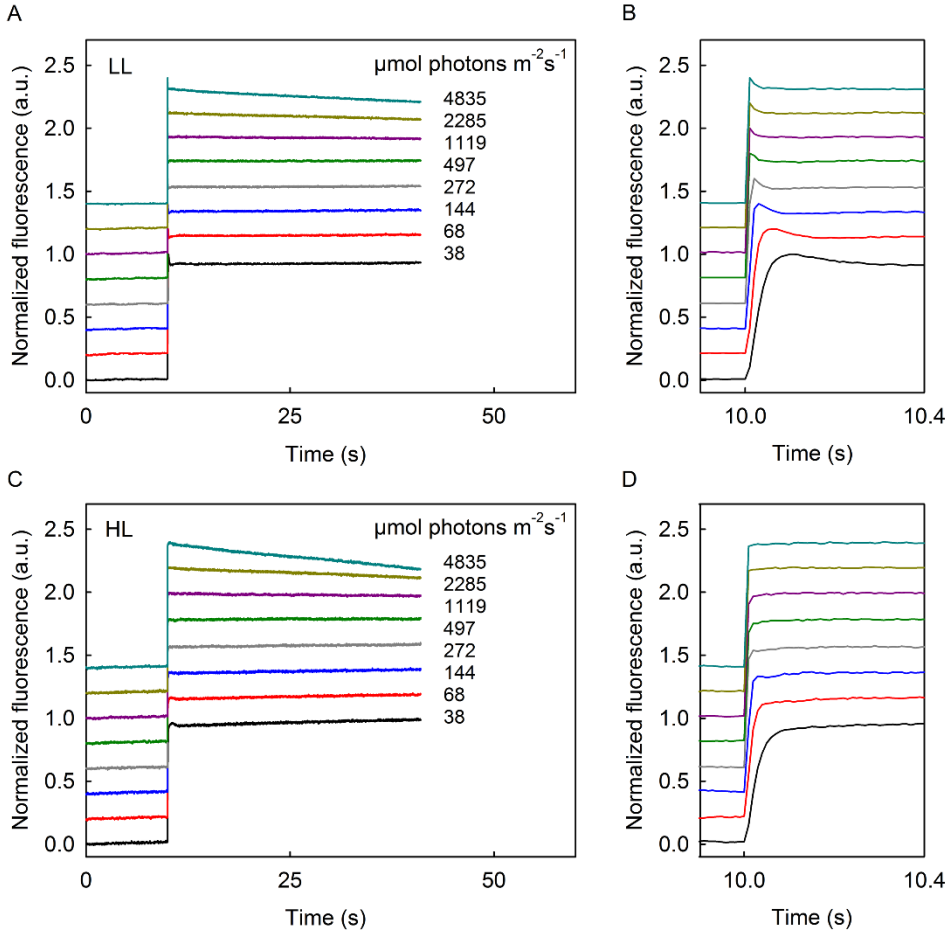

Fig. 7. Slow fluorescence kinetics in the presence of DCMU in a,b) low light and c,d) high light grown *P. tricornutum* cells. White actinic light was turned on at 10 s timepoint. PPFD values for each curve are as indicated in the figures. Panels b) and d) show the induction phase of each curve in more detail. All curves are averages from three biological replicates.

Appendix S1

Table S1. White growth light lamps used for different species.

Species	White light source
Acetabularia acetabulum	Philips TL-D 58W/840 fluorescent lamp (Philips, Amsterdam, Netherlands)
Arabidopsis thaliana	Philips TL-D 36W/840 fluorescent lamp (Philips, Amsterdam, Netherlands)
Chlorella vulgaris	Philips TL-D 36W/840 fluorescent lamp (Philips, Amsterdam, Netherlands)
Cucurbita maxima	Philips Master HPI-T plus 400W metal halide lamp (Philips, Amsterdam, Netherlands)
Phaeodactylum tricornutum low light	Osram Dulux intelligent longlife 18W fluorescent lamp (Osram, Munich, Germany)
Phaeodactylum tricornutum high light	Algaetron AG 230-ECO LED lamps (Photon Systems Instruments, Drasov, Czech Republic)
Synechocystis sp. PCC 6803	Philips TL-D 36W/865 fluorescent lamp (Philips, Amsterdam, Netherlands)
Vaucheria litorea	Philips TL-D 36W/840 fluorescent lamp (Philips, Amsterdam, Netherlands)

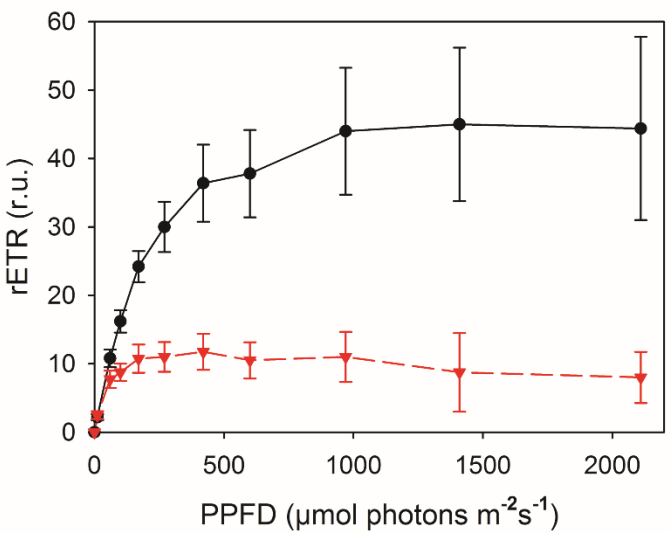

Fig. S1. RLCs measured from *Vaucheria litorea* (black solid line, circles) and *Acetabularia acetabulum* (red dashed line, triangles) using PAM-2000 with 30 s illumination for each light intensity step. Each data point represents an average of three independent measurements and the error bars indicate SD.

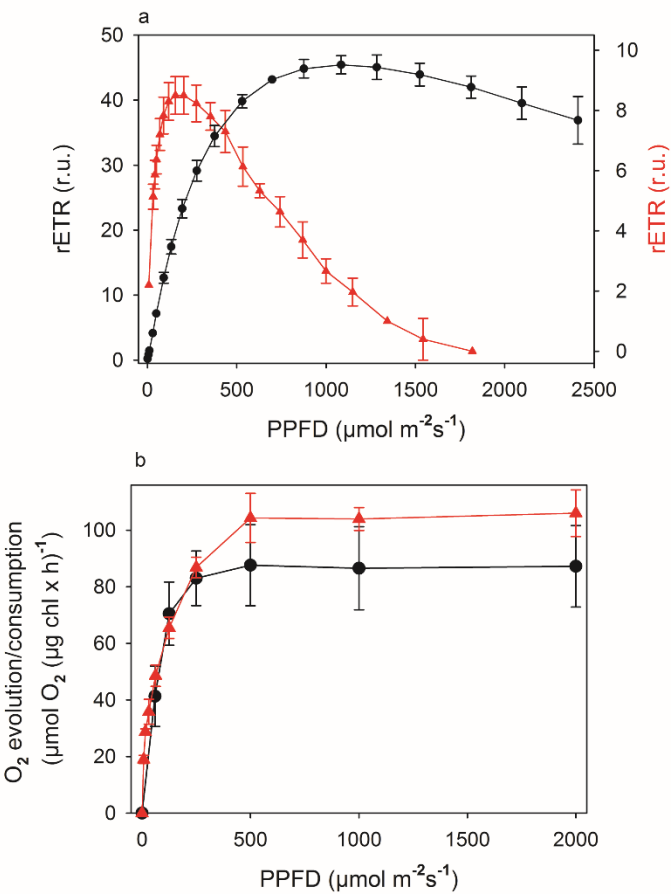

Fig. S2. Comparison of RLC and oxygen evolution measurements. a) Fluorescence based RLCs from *Synechocystis* (black circles) and isolated pumpkin thylakoids (red triangles). b) Light response of photosynthetic oxygen evolution of *Synechocystis* measured in fresh BG-11 supplemented with 10 mM bicarbonate (black circles) and of the full-chain electron transfer rate of isolated pumpkin thylakoids measured as oxygen consumption in the presence of 0.1 mM MV

(red triangles). Thylakoid measurements were performed in PSII measuring buffer. Each data point represents an average of three independent measurements and the error bars indicate SD.

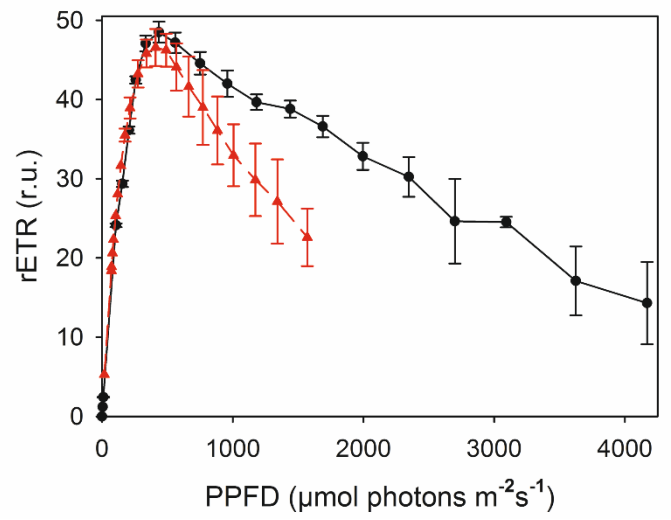

Fig. S3. Rapid light curve measured from *P. tricornutum* (black solid line, circles) and *C. vulgaris* (red dashed line, triangles) by detecting fluorescence at 680 nm. White actinic light was used. Each data point represents an average of three independent measurements and the error bars indicate SD.

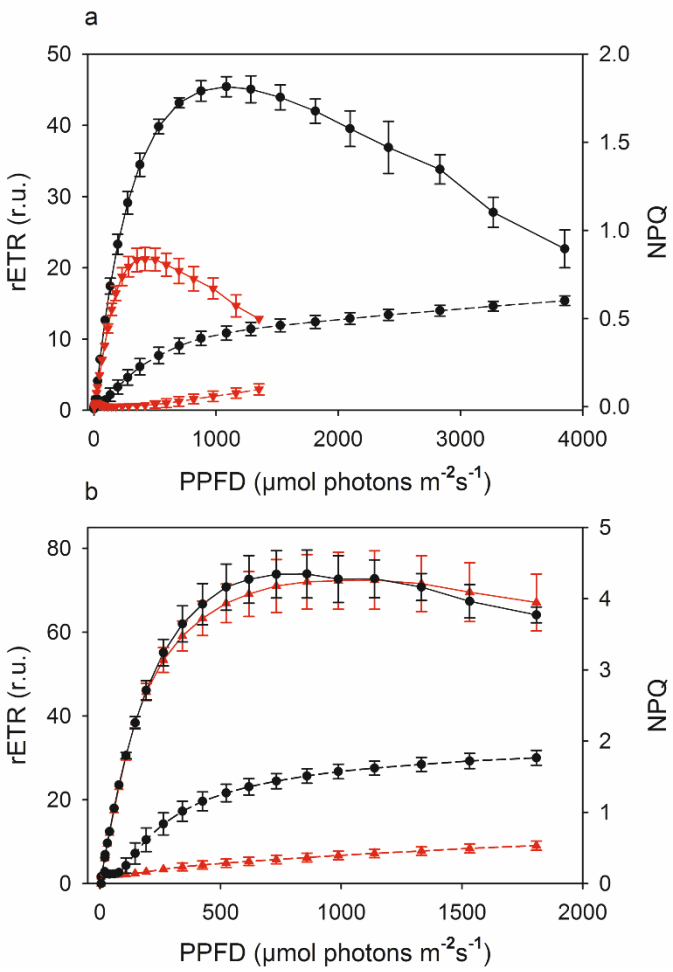

Fig. S4. Effect of NPQ on RLC measurements. a) RLC from *Synechocystis* using white (black circles, solid line) and orange (red triangles, solid line) actinic lights. The respective NPQ levels during the measurements are drawn with dashed lines bearing the same symbols. b) RLCs and NPQ from leaves of WT *A. thaliana* (black circles) and *npq1-2* mutant (red triangles) in white actinic light. NPQ was calculated as $[F_M - F_M']/F_M'$. All curves are averages from 3 independent replicates and the error bars indicate SD.

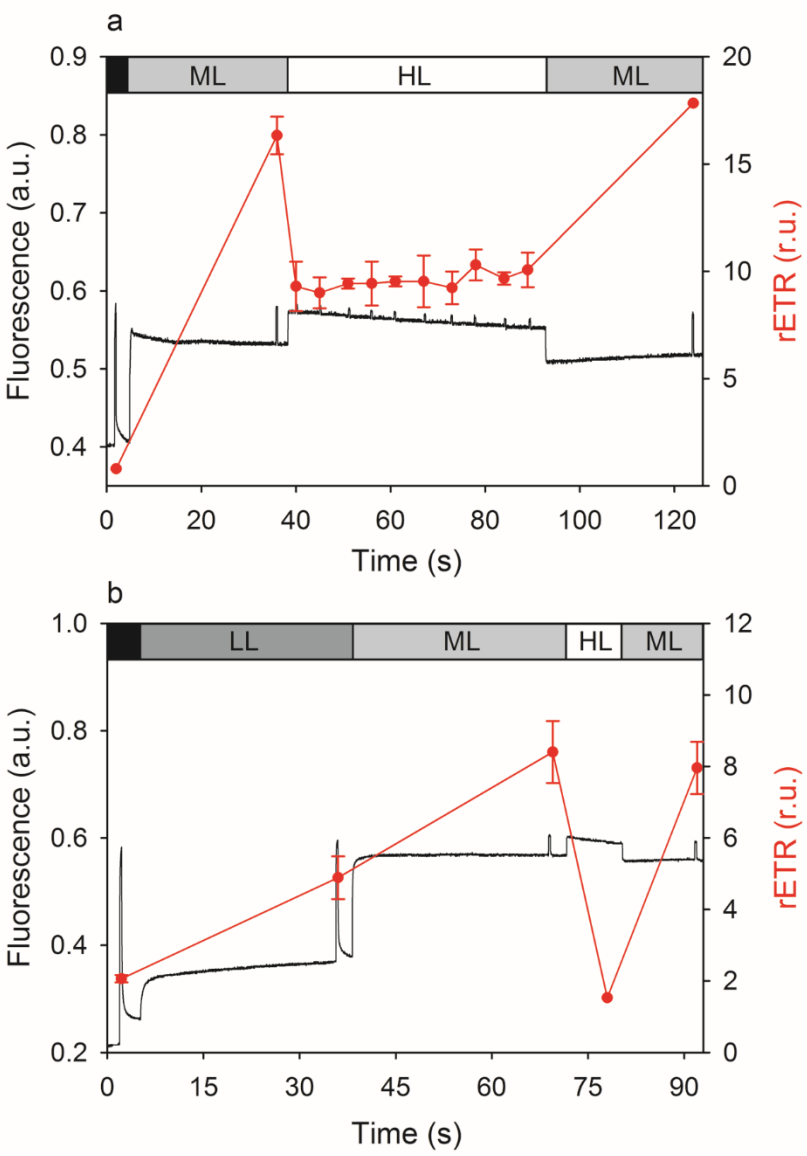

731

732 Fig. S5. Kinetics of rETR in *Synechocystis* in orange 590 nm light (a) and in isolated pumpkin
733 thylakoids in white light (b) during transitions to different light intensities. The bars on top of the
734 figures indicate darkness (black bar), low light (LL, PPFD 30 μmol $m^{-2}s^{-1}$, thylakoids only),
735 moderate light (ML, 450 or 350 μmol $m^{-2}s^{-1}$ for *Synechocystis* and for thylakoids, respectively)
736 and high light (HL, 1420 or 1820 μmol $m^{-2}s^{-1}$ for *Synechocystis* and for thylakoids, respectively).
737 *Synechocystis* fluorescence measurements were carried out in fresh BG-11 and thylakoid
738 measurements were performed in PSII measuring buffer in the presence of 0.1 mM MV.
739 Representative fluorescence traces are shown in black. Each rETR data point represents an
740 average of three independent replicates and error bars indicate SD.